ACS APPLIED MATERIALS & INTERFACES

RESEARCH ARTICLE

www.acsami.org

Fiber-like TiO_2 Nanomaterials with Different Crystallinity Phases Fabricated via a Green Pathway

Jian Zeng,[†,‡] Ran Li,[†] Shilin Liu,[†] and Lina Zhang*[,†]

[†]Department of Chemistry, Wuhan University, Wuhan 430072, China

[‡]Guangzhou Sugarcane Industry Research Institute, Guangdong Key Lab of Sugarcane Improvement & Biorefinery, Guangzhou 510316, China

ABSTRACT: Fiber-like TiO_2 nanomaterials were designed and created, for the first time, by in situ synthesis of TiO_2 nanoparticles in regenerated cellulose fibers in the wet state, followed by calcination at 400−800 °C to remove the cellulose matrix. The cellulose fibers were prepared in an NaOH/urea aqueous system with cooling via an industrial machine. The structure and properties of the fiber-like TiO_2 nanomaterials were characterized with scanning electron microscopy, transmission electron microscopy, X-ray diffraction, and photocatalytic degradation tests. The results revealed that the mean diameter of the fiber-like TiO_2 nanomaterials, which consisted of TiO_2 nanoparticles with a mean size from 21 to 37 nm, was 7−8 μm. The TiO_2 nanomaterials exhibited different crystallinity phases from anatase to rutile, depending on the calcinating temperature. With a decrease in the calcinating temperature from 800 to 400 °C, the surface area of the TiO_2 nanomaterials increased. The photocatalytic activity for the degradation of methyl orange of the anatase T-400 fibers calcined at 400 °C was the highest, compared with that at 600 and 800 °C. This work provided a simple and "green" pathway for the preparation of inorganic nanomaterials with different crystal structures by using porous regenerated cellulose matrix.

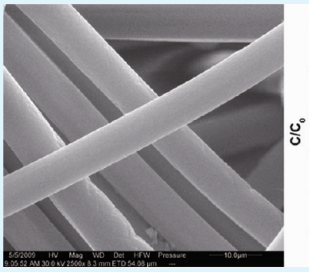

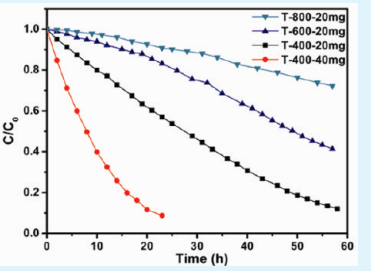

KEYWORDS: crystal structures, cellulose matrix, fiber-like TiO_2 nanomaterials, photocatalytic activity

INTRODUCTION

Metal oxide nanomaterials have received much attention due to their unique physical properties and potential applications in nanoelectronics, catalysts, sensors, and optical devices. Among oxide metals, TiO_2 nanomaterials have shown promising physical properties for various applications in photoelectronic activity, solar energy conversion, and photocatalysis for self-cleaning surface, air, and water purification.[1−4] TiO_2 has been proved to be the most excellent photocatalyst for the oxidative degradation of organic compounds under ultraviolet (UV) irradiation. Many organic pollutants, such as alcohols, phenols, dyes, and carboxylic acids, can be effectively photodegraded by TiO_2 nanomaterials under UV light irradiation.[5−7] Several techniques have been developed for the fabrication of TiO_2 nanomaterials, such as hydrothermal synthesis, self-assembly, electrospinning, and template growth.[8−11] Biological templates such as wood and natural cellulose fibers have been used to prepare inorganic nanomaterials recently.[12−15] However, facile and low-cost as well as "green" physicochemical methods for the preparation of the fiber-like TiO_2 nanomaterials have been scarcely reported.

In our laboratory, a novel solvent of 7.0 wt % NaOH/12.0 wt % urea aqueous solutions precooled to −12 °C has been developed to dissolve cellulose. Moreover, regenerated cellulose films and fibers with good structure and properties have been prepared successfully from the cellulose dope.[16,17] We have performed a high-efficiency, low-cost, and pollution-free process of primarily industrial spinning of the cellulose fiber.[18] It is worthy noting that the regenerated cellulose films and fibers in the wet state possess porous structure and hydroxyl groups and have been shown to be very useful for the creation of inorganic nanoparticles in the cellulose matrix.[19−21] On the basis of the porous structure of regenerated cellulose fibers in the wet state, iron oxide nanomaterials have been fabricated.[22] In the present study, we attempted to develop a simple method for the preparation of fiber-like TiO_2 nanomaterials with different crystals by calcination of regenerated cellulose fibers containing TiO_2 nanoparticles at various temperatures. The structure and properties of the fiber-like TiO_2 nanomaterials were characterized with X-ray diffraction, scanning electron microscopy, transmission electron microscopy, and photocatalytic degradation tests. This work would open up a completely new avenue for the design and fabrication of fiber-like TiO_2 nanomaterials by using regenerated natural polymer as templates.

EXPERIMENTAL SECTION

Materials. The cellulose (cotton linter pulp) with α-cellulose content of more than 95% was provided by the Jiujiang Chemical Fiber Co. Ltd. (Jiujiang, China). The viscosity-average molecular weight (M_w) of cellulose samples was determined to be 5.6×10^4 g·mol^{-1} (DP = 350) in LiOH/urea aqueous solution at 25 ± 0.05 °C.[23] All other chemical regents were of analytical grade and were used without further purification.

Received: March 9, 2011
Accepted: May 9, 2011
Published: May 09, 2011

dx.doi.org/10.1021/am200297b | *ACS Appl. Mater. Interfaces* 2011, 3, 2074–2079

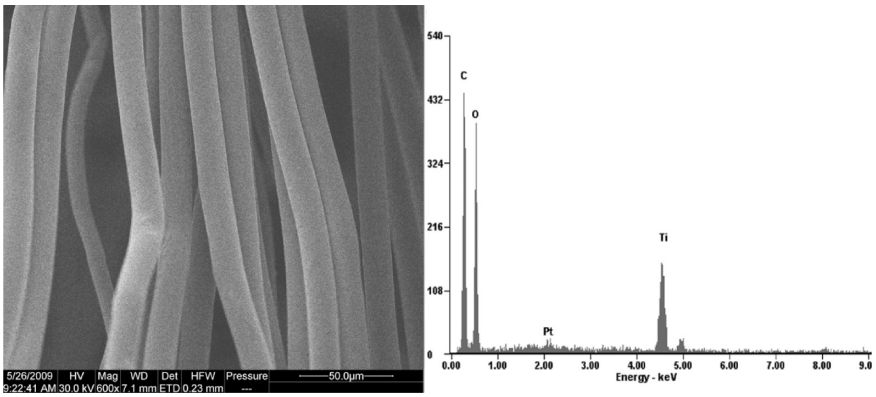

Figure 1. SEM image (left) and EDS spectrum (right) of the T6 composite fibers.

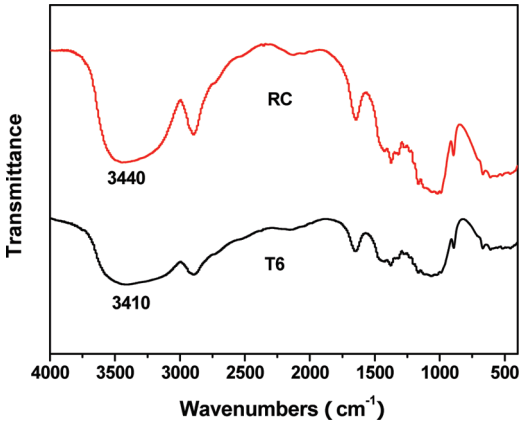

Figure 2. FT-IR spectra of the RC fibers and T6 composite fibers.

Preparation of Regenerated Cellulose Fibers. A mixture solution with NaOH/urea/H_2O of 7:12:81 by weight was precooled to −12 °C by a low-temperature cycle cooling system. Then, a cellulose sample with a desired amount was dispersed into the solvent system (1000 L) under vigorous stirring for 15 min at ambient temperature to obtain a transparent cellulose dope with concentrations of 5.2 wt %. The fibers were made by wet spinning on a pilot spinning machine manufactured by Jiangsu Longma Green Chemical Fiber Co. Ltd. (Haian, China).[18] The spinneret cylinder was immersed directly into the first coagulation bath with 15% H_2SO_4/10% Na_2SO_4, and the resulting gelation fibers solidified in the first coagulation bath were taken up on the first roller and then into the second coagulation bath with 5 wt % H_2SO_4. To wash out the residual salts and acid, the resultant fibers were put through a water bath until the pH value of the fibers was about 7 and then stretched by the third roller. The preparation of the regenerated cellulose fibers is a green process because the solvent is nontoxic and it maintains clean air during the production.[16−18]

Preparation of Fiber-like TiO_2 Nanomaterials. TiO_2 sol solution was prepared by mixing 20 mL of anhydrous ethanol, 20 mL of 1 M HNO_3, and a desired amount of tetrabutyl titanate ($Ti(OBu)_4$). Tetrabutyl titanate was added into the anhydrous ethanol under stirring, and then HNO_3 was added into the mixture solution under vigorous stirring for 20 min to obtain the TiO_2 sol solution at room temperature, which was a pale yellow, transparent solution.

The regenerated cellulose fibers were immersed into anhydrous ethanol for 60 min and then were immersed into TiO_2 sol solution for 2 h. The resultant TiO_2/cellulose composite fibers were washed by deionized water for 24 h. Finally, the composite fibers were dried at ambient conditions. The TiO_2/cellulose composite fibers treated with TiO_2 sol solution having the volume of tetrabutyl titanate of 4, 6, 8, and 10 mL were coded as T4, T6, T8, and T10, respectively. The pure cellulose fibers that were not treated with TiO_2 sol solution was coded as RC. The T6 composite fibers were calcined at 400, 600, 700, and 800 °C under air atmosphere for 3 h in a muffle to obtain fiber-like TiO_2 nanomaterials, and the resulting samples were coded as T-400, T-600, T-700, and T-800, respectively.

Characterization. Scanning electron microscopy (SEM) measurements were carried out on a SEM (SEM, Hitachi S-470, Japan) by using an accelerating voltage of 20 kV. The samples were coated with Pt for the SEM observation. Transmission electron microscopy (TEM) images were obtained on a JEOL JEM-2010 (HT) electron microscope, using an accelerating voltage of 200 kV. The samples for the TEM observation were prepared by ultrasonically dispersing the TiO_2 fibers in ethanol. Wide-angle X-ray diffraction (XRD) measurement was carried out on a XRD diffractometer (D8-Advance, Bruker, USA). The samples of composite fibers were ground into powders to remove the influence from the crystalline orientation of each fiber sample. The patterns with Cu Kα radiation (λ = 0.15406 nm) at 40 kV and 40 mA were recorded in the region of 2θ from 5 to 60° with a step speed of 2°/min. Thermal gravimetric analysis (TGA) was carried out on a Netzsch thermogravimetric analyzer (Germany). The dry composite fibers were ground into powder, and then the sample was placed in a platinum pan and heated from 30 to 600 °C at a rate of 10 K/min under air atmosphere. Nitrogen adsorption−desorption measurements were performed by using an ASAP 2020 (Micromeritics, USA) volumetric adsorption apparatus.

Photocatalytic Degradation of Methyl Orange. The photocatalytic activity of the fiber-like TiO_2 nanomaterials was assessed by monitoring the degradation of methyl orange. Twenty milligrams of the fiber-like TiO_2 nanomaterials was immersed into a 20 mL 10.5 mg/L (32 μM) methyl orange aqueous solution in the dark for 6 h. Subsequently, the solution with the fiber-like TiO_2 nanomaterials was irradiated under 6 W UV light (Gucun, Shanghai) at a wavelength of 254 nm. The mean light intensity of the UV light was measured with a power meter about 0.56 mW/cm^2. The concentration of methyl orange was monitored by detecting the UV absorbance intensity at 462 nm at given irradiation time intervals. The methyl orange UV absorbance was carried out on a UV−visible spectrometer (UV-160A, Shimadzu, Japan). The percentage of degradation was reported as C/C_0. Here C is the absorption of methyl orange at each irradiated time interval of the main peak of the absorption spectrum at 462 nm, and C_0 is the absorption of the starting concentration when adsorption−desorption equilibrium is achieved.

RESULTS AND DISCUSSION

Creation of TiO_2 Nanoparticles in Cellulose Matrix. The SEM image and energy-dispersive spectrum (EDS) of the

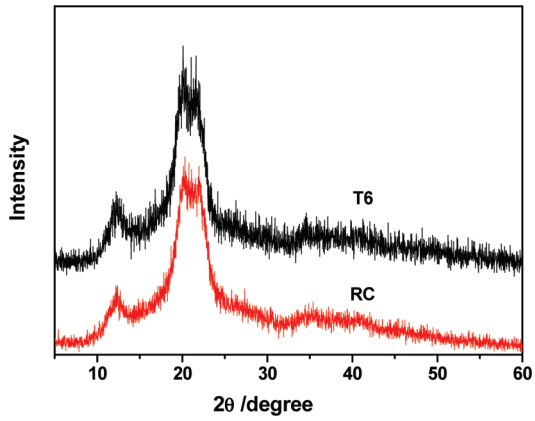

Figure 3. XRD patterns of the RC fibers and T6 composite fibers.

TiO_2/cellulose composite fibers from SEM are shown in Figure 1. It was indicated that there were C, O, and Ti elements in the composite fibers, suggesting that the TiO_2 nanoparticles have been synthesized in the cellulose fibers. The composite fibers exhibited a smooth surface. Therefore, the TiO_2/cellulose composite fibers were successfully fabricated by in situ synthesis in the porous cellulose matrix.

Figure 2 shows the FT-IR spectra of the RC fibers and the TiO_2/cellulose composite fibers. The peaks at 3300−3450 cm^{-1} corresponding to stretching vibrations of the hydroxyl groups of cellulose in the composite fibers shifted to lower wavenumbers, indicating a strong interaction between the hydroxyl groups of cellulose and the TiO_2 particles through hydrogen bonding interactions. This strong interfacial interaction led to the immobilization of TiO_2 nanoparticles in the cellulose matrix. Figure 3 shows the XRD patterns of the RC fibers and the composite fibers. The peaks at 2θ = 12.1, 20.3, and 21.8° are corresponding to the $(1\bar{1}0)$, (110), and (200) planes of cellulose II crystalline, respectively.[24] It was noted that, in addition to the peaks of cellulose II, the composite fibers did not display any TiO_2 crystalline peaks, such as those of anatase and rutile crystallines, clearly. It suggested that the TiO_2 nanoparticles in the composite fibers existed in an almost amorphous state.[25,26]

The thermal stability of the RC fibers and the TiO_2/cellulsoe composite fibers (T6) is shown in Figure 4. A small weight loss observed at 70−130 °C was attributed to the release of moisture from the samples. The thermal stability of the RC fibers decreased with the loading of TiO_2 particles. The decomposition temperature of the composite fibers was lower than 300 °C, which was lower that that of the RC fibers (300 °C). This was a result of the catalytic property of the incorporated inorganic nanoparticles.[27] From the TG data, the content of TiO_2 nanoparticles in the composite fibers was calculated to be 17.5, 21.6, 26.1, and 30.6 wt % for the T4, T6, T8, and T10 composite fibers, respectively. This indicated that the content of TiO_2 nanoparticles in the composite fibers was very high and the interfacial interaction between TiO_2 nanoparticles and cellulose matrix was strong.

Structure of Fiber-like TiO_2 Nanomaterials. Figure 5 shows the photographs of the TiO_2/cellulsoe composite fibers (T6) and the fiber-like TiO_2 nanomaterials (T-400). It was clearly shown that the cellulose matrix has been decomposed completely to display the white TiO_2 fibers. After the removal of the cellulose matrix by calcination, the resultant TiO_2 nanomaterials maintained fiber morphology. Figure 6 shows the SEM images of

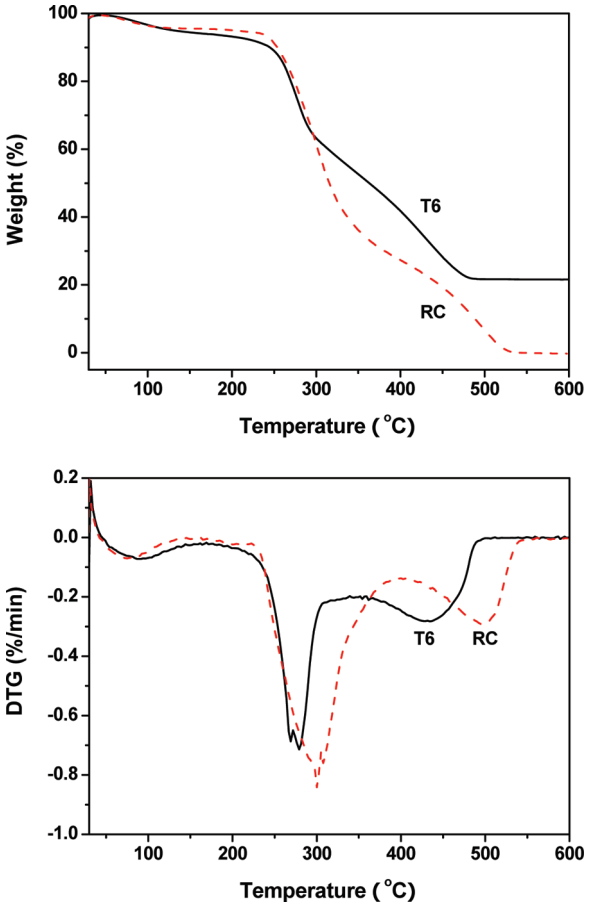

Figure 4. Thermogravimetric (TG) and differential thermogravimetric (DTG) curves of the RC fibers and T6 composite fibers under air atmosphere.

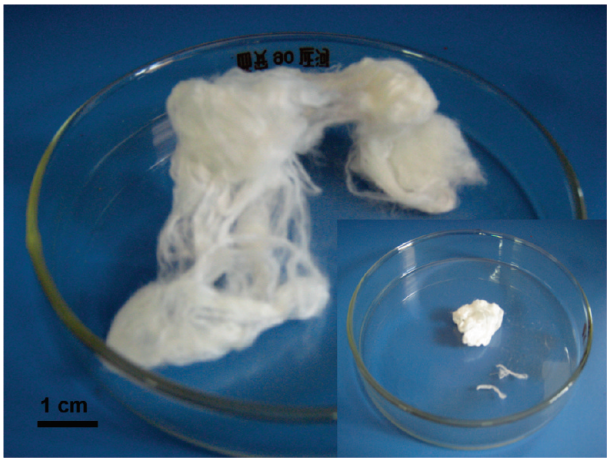

Figure 5. Photographs of the T6 composite fibers and T-400 of the fiber-like TiO_2 nanomaterials (inset).

the T6 composite fibers and fiber-like TiO_2 nanomaterials. The mean diameter of the TiO_2/cellulose composite fibers at the dry state was about 18 μm, and the mean diameter of the TiO_2 fibrous nanomaterials was about 7−8 μm. The reduced size of the fiber-like TiO_2 nanomaterials could be a result of the

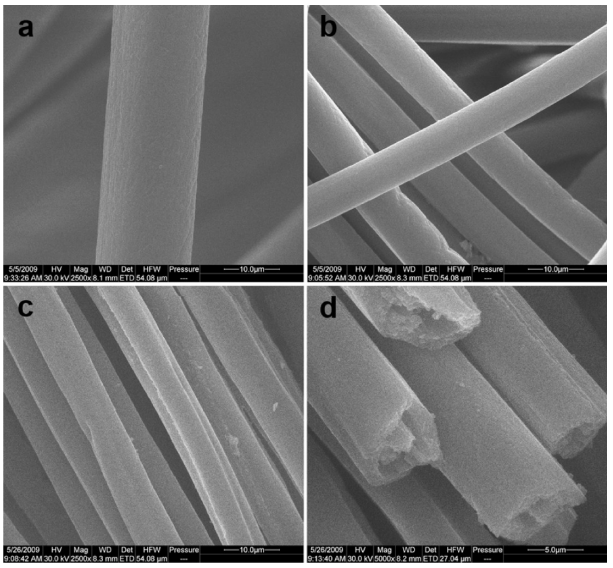

Figure 6. SEM images of the T6 composite fibers (a), as well as T-400 fibers (b), T-600 fibers (c), and T-800 fibers (d).

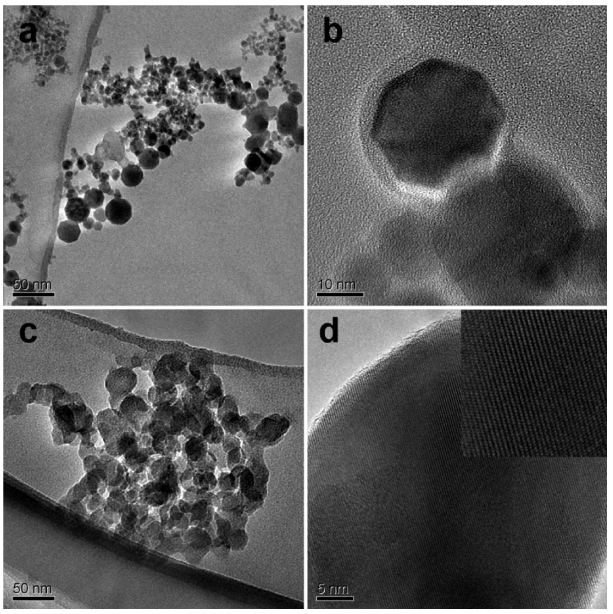

Figure 7. TEM images of the T-400 (a,b), T-600 (c), and T-800 (d) fibers.

calcination of the cellulose matrix.[22] The T4, T8, and T10 composite fibers were similarly calcined at 400, 600, and 800 °C under air atmosphere for 3 h also to obtain fiber-like TiO_2 nanomaterials. Therefore, it indicated that the content of TiO_2 nanoparticles in the composite fibers had no effect on TiO_2 fiber formation in this work. This method is easy and cost-effective, and the fiber-like TiO_2 samples could be fabricated on a large scale. The main advantage of this approach is the low amounts of waste, which may be seen as a green pathway.

The TEM images of TiO_2 fibers are shown in Figure 7. Clearly, the fiber-like TiO_2 nanomaterials were composed of pure TiO_2 nanoparticles. Interestingly, an increase in the calcinating temperature caused the grains to grow. The mean size (diameter) of

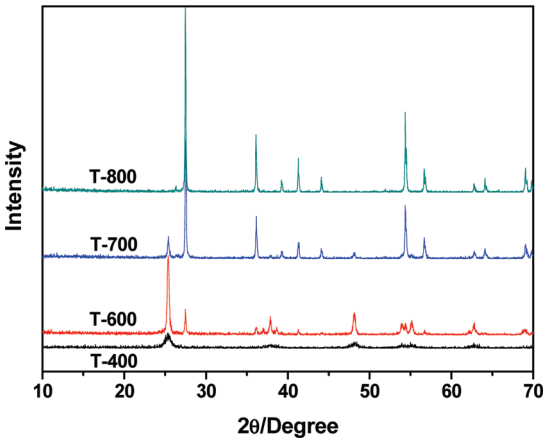

Figure 8. XRD patterns of the fiber-like TiO_2 nanomaterials calcined at different temperatures.

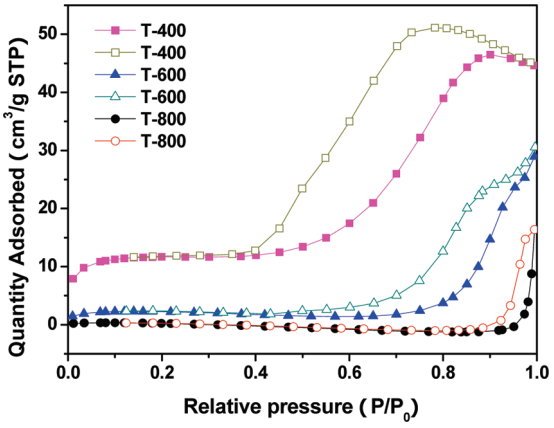

Figure 9. Nitrogen adsorption (solid) and desorption (open) isotherms of the fiber-like TiO_2 nanomaterials calcined at different temperatures.

the TiO_2 nanoparticles was 21, 30, and 37 nm for the T-400, T-600, and T-800 fibers, respectively.

The phase evolution and crystal structure of the fiber-like TiO_2 nanomaterials were studied using XRD techniques. Figure 8 shows the XRD patterns of the TiO_2 nanoparticles in the fibers. As mentioned above, the TiO_2 nanoparticles in the composite fibers were amorphous. However, well-crystallized pure anatase TiO_2 nanomaterials without any cellulose were obtained by calcination at 400 °C under air atmosphere for 3 h. Cellulose was decomposed completely in this case, and the amorphous TiO_2 transformed to anatase TiO_2 during calcination at 400 °C. The presence of the rutile phase was revealed in the XRD spectrum through the presence of a separate set of peaks that could be indexed to the rutile TiO_2. The fiber-like TiO_2 nanomaterials were in an anatase and rutile mixed phase at 600 and 700 °C. An increase in the calcinating temperature could enhance the volume fraction of the rutile phase as judged from the relative areas of the peaks corresponding to the anatase and rutile phases.[8] The TiO_2 nanoparticles in the fibers were almost pure rutile at 800 °C. It was noted that the calcinating temperature determined the crystallinity phase of the TiO_2 nanomaterials. Thus, by changing the calcinating temperature,

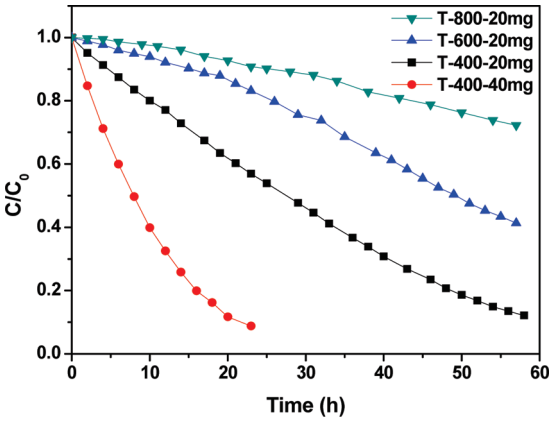

Figure 10. Photodegradation curves of methyl orange with the fiber-like TiO_2 nanomaterials calcined at different temperatures.

we can control the crystallinity phase of the fiber-like TiO_2 nanomaterials.

Figure 9 shows the nitrogen adsorption and desorption isotherms of the fiber-like TiO_2 nanomaterials calcinated at different temperature.[22] The BET surface area of the T-400, T-600, and T-800 fibers was about 39.73, 7.33, and 0.58 m^2/g, respectively. The T-400 fibers possessed large surface area. Moreover, the BET surface area of the fiber-like TiO_2 nanomaterials decreased, and their packing density of TiO_2 increased with an increase in the calcinating temperature.

Photocatalytic Activities of Fiber-like TiO_2 Nanomaterials. The photocatalytic activity of the fiber-like TiO_2 nanomaterials calcinated at different temperatures was evaluated by the photodegradation of methyl orange under UV irradiation. Methyl orange was selected as a model pollutant. Temporal changes in the concentration of methyl orange were monitored by examining the variations in the maximal absorption in UV−vis spectra at 462 nm.[28−31] The photocatalytic activity of the TiO_2 nanomaterials under weak UV light irradiation was studied. The photodegradation curves of methyl orange by using the TiO_2 nanomaterials are shown in Figure 10. The intensity of the weak UV light (254 nm) was only 0.54 mW/cm^2. Usually, the photocatalytic activity of a catalyst is dependent on its crystallinity, crystallinity phase, and particle size. The high crystallinity and large surface area of a photocatalyst could effectively increase its photocatalytic activity.[32,33] In our findings, the photocatalytic activity for the degradation of methyl orange by using the T-400 fibers was the highest, compared with that calcinated at 600 and 800 °C. Namely, the photocatalytic activity of the anatase TiO_2 nanomaterials was much higher than the rutile TiO_2 nanomaterials. An increase in the calcinating temperature could decrease the photocatalytic activity of the TiO_2 nanomaterials as a result of the increased mean size of the TiO_2 nanoparticles. This result was supported by the results of TEM, XRD, and BET.

CONCLUSION

The regenerated TiO_2/cellulose composite fibers were fabricated successfully by in situ synthesis of TiO_2 nanoparticles in the regenerated cellulose matrix via a sol−gel method. A strong interfacial interaction led to the immobilization of TiO_2 nanoparticles in the cellulose matrix. The porous structure of regenerated cellulose fibers supplied not only a microreactor for the creation of TiO_2 nanoparticles but also a shell to prevent their aggregation. After calcination of the TiO_2/cellulose composite fibers, pure fiber-like TiO_2 nanomaterials with a size of 21−37 nm were created. The TiO_2 nanomaterials exhibited different crystallinity phases from anatase to rutile, depending on the calcinating temperature from 400 to 800 °C. The photocatalytic activity for the degradation of methyl orange by using the anatase T-400 fibers calcined at 400 °C was higher than others. Herein, we opened up a new avenue for creation of fiber-like TiO_2 nanomaterials via a simple and "green" process.

AUTHOR INFORMATION

Corresponding Author

*Phone: +86-27-87219274. Fax: +86-27-68762005. E-mail: lnzhang@public.wh.hb.cn.

ACKNOWLEDGMENT

This work was supported by National Basic Research Program of China (973 Program, 2010CB732203), and the National Natural Science Foundation of China (20474048 and 20874079).

REFERENCES

(1) Chen, X.; Mao, S. *Chem. Rev.* **2007**, 2891–2959.
(2) Wold, A. *Chem. Mater.* **1993**, *5*, 280–283.
(3) Tada, H.; Ishida, T.; Takao, A.; Ito, S. *Langmuir* **2004**, *20*, 7898–7900.
(4) Jin, M.; Zhang, X.; Nishimoto, S.; Liu, Z.; Tryk, D.; Emeline, A.; Murakami, T.; Fujishima, A. *J. Phys. Chem. C* **2007**, *111*, 658–665.
(5) Blount, M. C.; Kim, D. H.; Falconer, J. L. *Environ. Sci. Technol.* **2001**, *35*, 2988–2994.
(6) Tayade, R.; Kulkarni, R.; Jasra, R. *Ind. Eng. Chem. Res.* **2006**, *45*, 922–927.
(7) Liu, Z.; Zhang, X.; Nishimoto, S.; Jin, M.; Tryk, D.; Murakami, T.; Fujishima, A. *J. Phys. Chem. C* **2008**, *112*, 253–259.
(8) Kumar, A.; Jose, R.; Fujihara, K.; Wang, J.; Ramakrishna, S. *Chem. Mater.* **2007**, *19*, 6536–6542.
(9) Wang, F.; Liu, C.; Liu, C.; Chao, J.; Lin, C. *J. Phys. Chem. C* **2009**, *113*, 13832–13840.
(10) Formo, E.; Lee, E.; Campbell, D.; Xia, Y. *Nano Lett.* **2008**, *8*, 668–672.
(11) Chuangchote, S.; Jitputti, J.; Sagawa, T.; Yoshikawa, S. *ACS Appl. Mater. Interfaces* **2009**, *1*, 1140–1143.
(12) Huang, J.; Kunitake, T. *J. Am. Chem. Soc.* **2003**, *125*, 11834–11835.
(13) Huang, J.; Kunitake, T.; Onoue, S. *Chem. Commun.* **2004**, 1008–1009.
(14) Kemell, M.; Pore, V.; Ritala, M.; Leskela, M.; Linden, M. *J. Am. Chem. Soc.* **2005**, *127*, 14178–14179.
(15) Kim, Y.; Ribeiro, L.; Maillot, F.; Ward, O.; Eichhorn, S.; Meldrum, F. *Adv. Mater.* **2010**, *22*, 2082–2086.
(16) Qi, H.; Chang, C.; Zhang, L. *Green Chem.* **2009**, *11*, 177–184.
(17) Cai, J.; Zhang, L.; Zhou, J.; Qi, H.; Chen, H.; Kondo, T.; Chen, X.; Chu, B. *Adv. Mater.* **2007**, *19*, 821–825.
(18) Li, R.; Chang, C.; Zhou, J.; Zhang, L.; Gu, W.; Li, C.; Liu, S.; Kuga, S. *Ind. Eng. Chem. Res.* **2010**, *49*, 11380–11384.
(19) Rollins, H.; Lin, F.; Johnson, J.; Ma, J.; Liu, J.; Tu, M.; DesMarteau, D.; Sun, Y. *Langmuir* **2000**, *16*, 8031–8036.
(20) Liu, S.; Zhang, L.; Zhou, J.; Wu, R. *J. Phys. Chem. C* **2008**, *112*, 4538–4544.
(21) Ke, D.; Liu, S.; Dai, K.; Zhou, J.; Zhang, L.; Peng, T. *J. Phys. Chem. C* **2009**, *113*, 16021–16026.
(22) Liu, S.; Zhang, L.; Zhou, J.; Xiang, J.; Sun, J.; Guan, J. *Chem. Mater.* **2008**, *20*, 3623–3628.

(23) Cai, J.; Liu, Y.; Zhang, L. *J. Polym. Sci., Part B: Polym. Phys.* **2006**, *44*, 3093–3101.
(24) Togawa, E.; Kondo, T. *J. Polym. Sci., Part B: Polym. Phys.* **1999**, *37*, 451–459.
(25) Liu, J.; Nakamura, Y.; Ogura, T.; Shibasaki, Y.; Ando, S.; Ueda, M. *Chem. Mater.* **2008**, *20*, 273–281.
(26) Zeng, J.; Liu, S.; Cai, J.; Zhang, L. *J. Phys. Chem. C* **2010**, *114*, 7806–7811.
(27) Ma, Z.; Li, F.; Bai, H. *Propellants, Explos., Pyrotech.* **2006**, *31*, 447–451.
(28) Smith, Y.; Kar, A.; Subramanian, V. *Ind. Eng. Chem. Res.* **2009**, *48*, 10268–10276.
(29) Xu, Y.; Zhuang, Y.; Fu, X. *J. Phys. Chem. C* **2010**, *114*, 2669–2676.
(30) Yan, S.; Li, Z.; Zou, Z. *Langmuir* **2010**, *26*, 3894–3901.
(31) Kislov, N.; Lahiri, J.; Verma, H.; Goswami, Y.; Stefanakos, E.; Batzill, M. *Langmuir* **2009**, *25*, 3310–3315.
(32) Baiju, K.; Shukla, S.; Sandhya, K.; James, J.; Warrier, K. *J. Phys. Chem. C* **2007**, *111*, 7612–7622.
(33) Sun, M.; Li, D.; Li, W.; Chen, Y.; Chen, X.; He, Y.; Fu, X. *J. Phys. Chem. C* **2008**, *112*, 18076–18081.